Disturbance Rejection Adaptive Control for Atmospheric Effects on Aircraft

Wang Xin, *Chen Xin* *, *Wen Liyan*

College of Automation and Engineering, Nanjing University of Aeronautics and Astronautics, Nanjing 210016, P. R. China

(Received 22 October 2016; revised 26 March 2016; accepted 6 April 2017)

Abstract: Disturbance rejection algorithm based on model reference adaptive control (MRAC) augmentation is investigated for uncertain turbulence disturbances. A stable adaptive control scheme is developed based on lower diagonal upper (LDU) decomposition of the high frequency gain matrix, which ensures closed-loop stability and asymptotic output tracking. Under the proposed control techniques, the bounded stability is achieved and the controller is able to remain within tight bounds on the matched and unmatched uncertainties. Finally, simulation studies of a linearized lateral-directional dynamics model are conducted to demonstrate the performance of the adaptive scheme.

Key words: adaptive control; disturbance rejection; LDU decomposition; tracking performance

CLC number: V249.1 **Document code**: A **Article ID**: 1005-1120(2017)06-0637-10

0 Introduction

Several disturbance attenuation and rejection approaches have been established during the past decades. The H_∞ control technique which has advantages over classical ones is an effective disturbance attenuation method and has already been successfully applied in practice[1]. However, the robustness against disturbance achieved by the H_∞ control approach is guaranteed at the price of degraded nominal performance and the disturbance is assumed to have finite energy. Slide mode control is an effective robust control algorithm since it is insensitive to model uncertainties, external disturbances and parameter variations[2-4]. In Ref. [5], a method that combines H_∞ and integral sliding mode control was proposed. The main idea is to choose such a projection matrix, ensuring that unmatched perturbations are not amplified and moreover minimized. However, the slide mode control method has an inherent feature of the chattering phenomenon caused by the high-frequency control switching. This chattering could severely deteriorate the performance of the system.

Adaptive control systems are capable of tolerating large parametric, structural and parameterizable disturbance uncertainties, to ensure desired system asymptotic tracking performance, in addition to system stability[6]. Such asymptotic tracking performance is crucial to many performance-critical system applications like aircraft control systems. Some adaptive control methods with optimal control design were promoted to solve the disturbance problem[7-10]. In Ref. [11], the dead-zone modification stopped the adaptation process when the norm of the tracking error became smaller than the prescribed value[12]. However, the dead-zone modification was not lipschitz and it might cause high-frequency and other undesirable effects, especially when the tracking error was near the dead-zone boundary. The σ-modification together with a dynamic normalization was employed in the adaptive law to ensure robustness

* Corresponding author, E-mail address: chenxin@nuaa.edu.cn.

How to cite this article: Wang Xin, Chen Xin, Wen Liyan. Disturbance rejection adaptive control for atmospheric effects on aircraft[J]. Trans. Nanjing Univ. Aero. Astro., 2017,34(6):637-646.
http://dx.doi.org/10.16356/j.1005-1120.2017.06.637

for small tracking errors and e-modification was introduced to replace the constant damping gain σ with a term proportional to a linear combination of the system tracking errors[13,14].

However, for large tracking errors, the dead zone, the σ modification, and the e-modification slow down the adaptation. In Refs. [15,16], the adaptive feedforward cancelation algorithms could be applied to reject such frequency-modulated disturbances, which were exactly equivalent to a set of compensators implementing the internal model principle. In Refs. [17—20], optimal control modification method was developed for systems with unmatched uncertainty using a predictor model for estimating the control input. However, the existing adaptive disturbance rejection designs are mainly for the matched disturbance rejection or for the unmatched disturbance rejection, but with certain difficulty of achieving the asymptotic output tracking performance.

The motivation for studying adaptive controller comes from the fact that it is still significant to develop a new disturbance rejection techniques to deal with unmatched input disturbances for the asymptotic output tracking performance. The main contributions of this paper is to propose MRAC with lower diagonal upper (LDU) decomposition-based controller for multivariable linear systems with unmatched input disturbances, including key design conditions in terms of system control and disturbance relative degrees, nominal plant-model matching control designs, adaptive law and stability analysis.

1 Problem Formulation and Preliminaries

1.1 Problem statement

The lateral-directional motion of a conventional aircraft derived in Ref. [21] can be described as

$$\begin{pmatrix}\dot{\varphi}\\ \dot{\beta}\\ \dot{p}\\ \dot{r}\end{pmatrix}=\begin{bmatrix}0 & 0 & 1 & 0\\ \dfrac{g}{V} & \dfrac{Y_\beta}{V} & \dfrac{Y_p}{V} & \dfrac{Y_r}{V}-1\\ 0 & L_\beta & L_p & Y_r\\ 0 & N_\beta & N_p & N_r\end{bmatrix}\begin{pmatrix}\varphi\\ \beta\\ p\\ r\end{pmatrix}+$$

$$\begin{pmatrix}0 & 0\\ \dfrac{Y_{\delta_a}}{V} & \dfrac{Y_{\delta_r}}{V}\\ L_{\delta_a} & L_{\delta_r}\\ N_{\delta_a} & N_{\delta_r}\end{pmatrix}\begin{bmatrix}\delta_a\\ \delta_r\end{bmatrix}+\begin{bmatrix}\boldsymbol{b}_{\varphi_w} & \boldsymbol{b}_{\beta_w}\end{bmatrix}\begin{bmatrix}\varphi_w & \beta_w\end{bmatrix}^{\mathrm{T}} \tag{1}$$

where the rudder δ_r primarily controls the yaw rate r and the sideslip angle β. The ailerons δ_a change roll rate p and the bank angle φ. L_p, N_p are the roll and the yaw moment with respect to the roll rate, $L_\beta N_\beta$ the roll and the yaw moment with respect to the sideslip angle, $L_p N_p$ the roll and the yaw moment with respect to the yaw rate, Y_β, Y_p, Y_r the side force derivatives with respect to the sideslip angle, the roll rate and the yaw rate, Y_{δ_a}, Y_{δ_r} the side force derivatives with respect to the aileron and the rudder deflection, N_{δ_r}, L_{δ_r} the yaw and the roll moment derivatives with respect to the rudder deflection angle, L_{δ_a}, N_{δ_a} the yaw and the roll moment derivatives with respect to the aileron deflection angle, φ_w and β_w the angle of bank and the sideslip angle due to disturbance, b_{φ_w} and b_{β_w} the parameter vectors of disturbance. This linear aircraft system model can be described in the following form

$$\begin{aligned}\dot{\boldsymbol{x}}(t)&=\boldsymbol{A}\boldsymbol{x}(t)+\boldsymbol{B}\boldsymbol{v}(t)+\boldsymbol{B}_d\boldsymbol{d}(t)\\ \boldsymbol{y}(t)&=\boldsymbol{C}\boldsymbol{x}(t)\end{aligned} \tag{2}$$

where $\boldsymbol{A}\in\boldsymbol{R}^{n\times n}$, $\boldsymbol{B}\in\boldsymbol{R}^{n\times M}$, $\boldsymbol{B}_d\in\boldsymbol{R}^{n\times p}$ and $\boldsymbol{C}\in\boldsymbol{R}^{M\times n}$ are constant and unknown, $\boldsymbol{d}(t)=[d_1(t),\cdots d_p(t)]^{\mathrm{T}}\in\boldsymbol{R}^p$ is the disturbance vector. The element $d_j(t)$ is characterized as

$$d_j(t)=d_{j0}(t)+\sum_{k=1}^{q_j}d_{jk}f_{jk}(t) \tag{3}$$

where $d_{j0}(t)$ and $d_{jk}(t)$ are some unknown constants, $f_{k0}(t)$ some known bounded continuous signal, $j=1,2,3,\cdots,p$; $k=1,2,3,\cdots,q_j$. Note that such a parameterizable disturbance feature is necessary for an adaptive compensation design to cancel the disturbance effect.

An augmentation control signal $\boldsymbol{v}(t)$ is introduced to cope with system parameter uncertainties. The state variable $\boldsymbol{x}(t)$ is available for measurement, the nominal state feedback controller with the disturbance rejection term is

$$\boldsymbol{v}(t)=\boldsymbol{v}^*(t)=\boldsymbol{K}_1^{*\mathrm{T}}\boldsymbol{x}(t)+\boldsymbol{K}_2^*\boldsymbol{r}(t)+\boldsymbol{K}_3^*(t) \tag{4}$$

where the nominal parameters $\boldsymbol{K}_1^{*\mathrm{T}}(t) \in \boldsymbol{R}^{M\times n}$, $\boldsymbol{K}_2^{*\mathrm{T}}(t) \in \boldsymbol{R}^{M\times M}$ are for the plant-model output matching, $\boldsymbol{K}_3^{*\mathrm{T}}(t) \in \boldsymbol{R}^{M}$ is used to cancel the effect of the disturbance. $\boldsymbol{d}(t)$ and $\boldsymbol{r}(t) \in \boldsymbol{R}^{M}$ are external reference input signals. The control objective is to design an adaptive controller $\boldsymbol{v}(t)$ so that the system (2) output state vector signal $\boldsymbol{y}(t)$ can asymptotically track a reference output vector signal $\boldsymbol{y}_m(t)$ generate from a chosen reference model

$$\boldsymbol{y}_m(t) = \boldsymbol{W}_m(s)[r](t) \tag{5}$$

where $\boldsymbol{W}_m(s) \in \boldsymbol{R}^{M\times M}$ is a stable transfer function matrix to be chosen as $\boldsymbol{W}_m(s) = \boldsymbol{\xi}_m^{-1}(s) \in \boldsymbol{R}^{M\times M}$ for the modified interactor matrix $\boldsymbol{\xi}_m(s)$ of $\boldsymbol{G}_p(s) = \boldsymbol{C}(s\boldsymbol{I}-\boldsymbol{A})^{-1}\boldsymbol{B}$. Note that in this paper, we use the notation $\boldsymbol{y} = \boldsymbol{G}(s)[v](t)$ to represent the output $\boldsymbol{y}(t)$ of a system, whose transfer matrix is $\boldsymbol{G}(s)$, and input is $\boldsymbol{v}(t)$ a convenient notation for adaptive control systems.

1.2 Preliminaries and assumptions

Lemma 1[22] For every real matrix with nonzero, leading principal minors can be uniquely factored as

$$\boldsymbol{K}_p = \boldsymbol{LDU} \tag{6}$$

where $\boldsymbol{L}$ is the unity lower triangular, $\boldsymbol{U}$ the unity upper triangular, and

$$\boldsymbol{D} = \mathrm{diag}\{d_1, d_2, \cdots, d_m\} = \mathrm{diag}\{\Delta_1, \Delta_2\Delta^{-1}, \cdots, \Delta_m\Delta_{m-1}^{-1}\} \tag{7}$$

Lemma 2[22] For any $M\times M$ strictly proper and full rank rational transfer matrix $\boldsymbol{G}(s)$, there exists a lower triangular polynomial matrix $\boldsymbol{\xi}_m(s)$ defined as the left interactor matrix of $\boldsymbol{G}(s)$ as

$$\boldsymbol{\xi}_m(s) = \begin{bmatrix} d_1(s) & 0 & 0 & 0 \\ h_{21}^m(s) & d_2(s) & 0 & 0 \\ \vdots & \vdots & \vdots & \vdots \\ h_{M1}^m(s) & h_{M2}^m(s) & \cdots & d_M(s) \end{bmatrix} \tag{8}$$

where $h_{ij}^m(s), j = 1,2,3,\cdots,M-1; i = 2,3,\cdots,M$, are some polynomials and $d_I(s)$ are any chosen monic stable polynomials such that the high-frequency gain matrix of $\boldsymbol{G}(s)$ defined as $\boldsymbol{K}_p = \lim\limits_{s\to\infty} \boldsymbol{\xi}_m(s)\boldsymbol{G}(s)$. From the baseline controller based system in Eq. (1), the control and disturbance transfer functions are obtained as $\boldsymbol{G}_p(s) = \boldsymbol{C}(s\boldsymbol{I}-\boldsymbol{A})^{-1}\boldsymbol{B}$ and $\boldsymbol{G}_d(s) = \boldsymbol{C}(s\boldsymbol{I}-\boldsymbol{A})^{-1}\boldsymbol{B}_d$ and are expressed in their left coprime polynomial matrix decompositions: $\boldsymbol{G}_p(s) = \boldsymbol{P}_l^{-1}(s)\boldsymbol{Z}_p(s)$ and $\boldsymbol{G}_d(s) = \boldsymbol{P}_l^{-1}(s)\boldsymbol{Z}_d(s)$, where $\boldsymbol{P}_l(s)$, $\boldsymbol{Z}_p(s) \in \boldsymbol{R}^{M\times M}$ and $\boldsymbol{Z}_d(s) \in \boldsymbol{R}^{M\times p}$ are some polynomial matrices.

Assumption 1 All zeros of $\boldsymbol{G}_p(s)$ are stable, and $(\boldsymbol{A}, \boldsymbol{B}, \boldsymbol{C})$ is stabilizable and detectable.

Assumption 2 $\boldsymbol{G}_p(s)$ is strictly proper with full rank and has a known modified interactor matrix $\boldsymbol{\xi}_m(s)$ such that $\boldsymbol{K}_p = \lim\limits_{s\to\infty}\boldsymbol{\xi}_m(s)\boldsymbol{G}_p(s)$ is finite and nonsingular (so that $\boldsymbol{W}_m(s) = \boldsymbol{\xi}_m^{-1}(s) \in \boldsymbol{R}^{M\times M}$ can be chosen as the transfer matrix for the reference model system).

Assumption 3 The leading principal minors of the high-frequency gain matrix $\boldsymbol{K}_p$ are nonzero, and their signs are known.

Assumption 4 The transfer matrix $\boldsymbol{Z}_p^{-1}(s)\boldsymbol{Z}_d(s)$ is proper.

Remark 1 Assumption 1 is for output matching and internal signal stability. Assumption 2 is for choosing the reference system model for adaptive control. Assumption 3 is for designing adaptive parameter update laws. Assumption 4 is the relative degree condition from the control input $\boldsymbol{v}(t)$ and the disturbance input $\boldsymbol{d}(t)$ to the output $\boldsymbol{y}(t)$

2 Adaptive Disturbance Rejection Design

2.1 Adaptive controller design

In this section, an adaptive rejection of unmatched input disturbances in multivariable systems is introduced to the augmentation of the baseline controller based on LDU decompositions of $\boldsymbol{K}_p$.

Lemma 3 The matrix $\boldsymbol{K}_d = \lim\limits_{s\to\infty}\boldsymbol{\xi}_m(s)\boldsymbol{G}_d(s)$ is finite if $\boldsymbol{Z}_p^{-1}(s)\boldsymbol{Z}_d(s)$ is proper.

Proof

From Assumption 2, $\boldsymbol{K}_p = \lim\limits_{s\to\infty}\boldsymbol{\xi}_m(s)\boldsymbol{G}_p(s)$ is finite and nonsingular. We have

$$\lim_{s\to\infty}\boldsymbol{K}_p^{-1}\boldsymbol{\xi}_m(s)\boldsymbol{G}_p(s) = \boldsymbol{I} \tag{9}$$

Hence, if $\boldsymbol{Z}_p^{-1}(s)\boldsymbol{Z}_d(s)$ is proper, $\boldsymbol{K}_p^{-1}\xi_m(s)\boldsymbol{Z}_p^{-1}(s)\cdot\boldsymbol{Z}_d(s)$ is proper, that is

$$\lim_{s\to\infty}\boldsymbol{K}_p^{-1}\boldsymbol{\xi}_m(s)\boldsymbol{G}_p(s)\boldsymbol{Z}_p^{-1}(s)\boldsymbol{Z}_d(s) < \infty \tag{10}$$

Using $\boldsymbol{G}_p(s)=\boldsymbol{P}_l^{-1}(s)\boldsymbol{Z}_p(s)$ in Eq. (10), we have

$$\lim_{s\to\infty}\boldsymbol{K}_p^{-1}\boldsymbol{\xi}_m(s)\boldsymbol{P}_l^{-1}(s)\boldsymbol{Z}_p(s)\boldsymbol{Z}_0^{-1}(s)\boldsymbol{Z}_d(s)=\lim_{s\to\infty}\boldsymbol{K}_p^{-1}\boldsymbol{\xi}_m(s)\boldsymbol{P}_l^{-1}(s)\boldsymbol{Z}_d(s)=\lim_{s\to\infty}\boldsymbol{K}_p^{-1}\boldsymbol{\xi}_m(s)\boldsymbol{G}_d(s)<\boldsymbol{I} \tag{11}$$

So that we obtain the following: $\boldsymbol{\xi}_m(s)\boldsymbol{C}\cdot(s\boldsymbol{I}-\boldsymbol{A})^{-1}\boldsymbol{B}_d$ is proper, that is $\boldsymbol{K}_d=\lim_{s\to\infty}\boldsymbol{\xi}_m(s)\cdot\boldsymbol{G}_d(s)$ is infinite.

Based on Lemma 3, the existence of a nominal controller for the system in Eq. (2) is established a follows.

Theorem 1 From the baseline controller based system in Eq. (2) in the unmatched disturbances, under Assumptions 1 and 4, there exists a state feedback control law, to make the roundedness of all closed-loop signals, disturbance rejection, and output tracking the reference $\boldsymbol{y}_m(t)$.

Proof

From the baseline controller based system in Eq. (2), the input-output form is obtained as

$$\boldsymbol{y}(t)=\boldsymbol{G}_p(s)[v](t)+\bar{\boldsymbol{y}}(t) \tag{12}$$

with $\boldsymbol{G}_p(s)=\boldsymbol{C}(s\boldsymbol{I}-\boldsymbol{A})^{-1}\boldsymbol{B}$ and $\bar{\boldsymbol{y}}(t)=\boldsymbol{G}_d(s)[d](t)=\boldsymbol{C}(s\boldsymbol{I}-\boldsymbol{A})^{-1}\boldsymbol{B}$. Operate the interactor matrix (a polynomial matrix) $\boldsymbol{\xi}_m(s)$ in the system in Eq. (2), $\dot{\boldsymbol{x}}(t)=\boldsymbol{A}\boldsymbol{x}(t)+\boldsymbol{B}\boldsymbol{v}(t)+\boldsymbol{B}_d\boldsymbol{d}(t),\boldsymbol{y}(t)=\boldsymbol{C}\boldsymbol{x}(t)$, to reach an expression of $\boldsymbol{\xi}_m(s)\ [y_m](t)$ in a possible form

$$\boldsymbol{\xi}_m(s)[y](t)=-\bar{\boldsymbol{K}}_0\boldsymbol{x}(t)+\bar{\boldsymbol{K}}_p\boldsymbol{v}(t)+\bar{\boldsymbol{K}}_{p1}\dot{\boldsymbol{v}}+\cdots+\bar{\boldsymbol{K}}_{pl0}v^{(l_0)}(t)+\bar{\boldsymbol{K}}_d\boldsymbol{d}(t)+\bar{\boldsymbol{K}}_{d1}\dot{d}(t)+\cdots+\bar{\boldsymbol{K}}_{dl1}\boldsymbol{d}^{(l1)}(t) \tag{13}$$

with some constant matrices $\bar{\boldsymbol{K}}_0\in\boldsymbol{R}^{M\times n}$, $\bar{\boldsymbol{K}}_p\in\boldsymbol{R}^{M\times M}$, $\bar{\boldsymbol{K}}_{pj}\in\boldsymbol{R}^{M\times M},j=1,2,\cdots,l_0;\bar{\boldsymbol{K}}_d\in\boldsymbol{R}^{M\times p}$, and $\bar{\boldsymbol{K}}_{dj}\in\boldsymbol{R}^{M\times p},j=1,2,\cdots,l_1$. For some integers l_0, $l_1\geqslant 0$. From Eqs. (2) and (12), we have

$$\boldsymbol{x}(s)=(s\boldsymbol{I}-\boldsymbol{A})^{-1}\boldsymbol{B}\boldsymbol{v}(s)+(s\boldsymbol{I}-\boldsymbol{A})^{-1}\boldsymbol{B}_d\boldsymbol{d}(s) \tag{14}$$

Expressing Eq. (13) in s domain and using Eq. (14), we have

$$\boldsymbol{\xi}_m(s)\boldsymbol{y}(s)=-\bar{\boldsymbol{K}}_0\ (s\boldsymbol{I}-\boldsymbol{A})^{-1}B\boldsymbol{v}(s)+\bar{\boldsymbol{K}}_p\boldsymbol{v}(s)+\bar{\boldsymbol{K}}_{p1}s\boldsymbol{v}(s)+\cdots+\bar{\boldsymbol{K}}_{pl_0}s^{l_0}\boldsymbol{v}(s)-\bar{\boldsymbol{K}}_0\ (s\boldsymbol{I}-\boldsymbol{A})^{-1}B_d\boldsymbol{d}(s)+\bar{\boldsymbol{K}}_d\boldsymbol{d}(s)+\bar{\boldsymbol{K}}_{d1}s\boldsymbol{d}(s)+\cdots+\bar{\boldsymbol{K}}_{dl_1}s^{l_1}\boldsymbol{d}(s) \tag{15}$$

From Assumption 2 that $\boldsymbol{K}_p=\lim_{s\to\infty}\boldsymbol{\xi}_m(s)\boldsymbol{G}_p(s)$ is finite and nonsingular and Assumption 4, $\boldsymbol{K}_{pj}=0,j=1,2,\cdots,l_0,\bar{\boldsymbol{K}}_p=\boldsymbol{K}_p$, and $\boldsymbol{K}_{dj}=0,j=1,2,\cdots,l_0,\bar{K}_d=\boldsymbol{K}_d,K$ hence, we have

$$\boldsymbol{\xi}_m(s)[y](t)=-\bar{\boldsymbol{K}}_0\boldsymbol{x}(t)+\boldsymbol{K}_p\boldsymbol{v}(t)+\boldsymbol{K}_d\boldsymbol{d}(t) \tag{16}$$

From Eq. (16) that the control law can be designed as

$$\boldsymbol{v}(t)=\boldsymbol{v}^*(t)=\boldsymbol{K}_1^{*\mathrm{T}}\boldsymbol{x}(t)+\boldsymbol{K}_2^*\boldsymbol{r}(t)+\boldsymbol{K}_3^*(t) \tag{17}$$

where $\boldsymbol{K}_1^{*\mathrm{T}}=\boldsymbol{K}_p^{-1}\bar{\boldsymbol{K}}_0,\boldsymbol{K}_2^*=\boldsymbol{K}_p^{-1}$ and $\boldsymbol{K}_3^*(t)=\boldsymbol{K}_{3d}\boldsymbol{d}(t)$ with $\boldsymbol{K}_{3d}(t)=-\boldsymbol{K}_p^{-1}\boldsymbol{K}_d$ which leads the output matching: $\boldsymbol{\xi}_m(s)\ [y_m](t)=\boldsymbol{r}(t)$. From the Eq. (17) to the system in Eq. (2), we have

$$\boldsymbol{y}(t)=\boldsymbol{C}(s\boldsymbol{I}-\boldsymbol{A}-\boldsymbol{B})-1\boldsymbol{B}\boldsymbol{K}_2^*[r](t)+\boldsymbol{C}(s\boldsymbol{I}-\boldsymbol{A}-\boldsymbol{B})-1\boldsymbol{B}[\boldsymbol{K}_3^*](t)+\boldsymbol{C}(s\boldsymbol{I}-\boldsymbol{A}-\boldsymbol{B})-1\boldsymbol{B}_d\boldsymbol{d}(s)=\boldsymbol{W}_m(s)[r](t)=\boldsymbol{y}_m(t) \tag{18}$$

Remark 2 From the Eq. (18), we can conclude that the plant-model matching conditions are

$$\boldsymbol{C}(s\boldsymbol{I}-\boldsymbol{A}-\boldsymbol{B})-1\boldsymbol{B}\boldsymbol{K}_2^*=\boldsymbol{W}_m(s)\boldsymbol{W}_m(s)\boldsymbol{K}_2^{*-1}$$
$$\boldsymbol{K}_3^*(s)+\boldsymbol{C}(s\boldsymbol{I}-\boldsymbol{A}-\boldsymbol{B})-1\boldsymbol{B}_d\boldsymbol{d}(s)=0 \tag{19}$$

2.2 Parameterizations of $K_3^{*\mathrm{T}}(t)$

For the disturbance vector $\boldsymbol{d}(t)\in\boldsymbol{R}^p$ each element $d_j(t)$ in Eq. (2) can be expressed as

$$d_j(t)=d_{j0}+\sum_{k=1}^{q_j}d_{jk}\boldsymbol{f}_{jk}(t)=\boldsymbol{\mu}_j^{*\mathrm{T}}\boldsymbol{f}_j(t)\quad j=1,2,\cdots,p \tag{20}$$

where the parameter matrix and the disturbance signal components are

$$\boldsymbol{\mu}_j^*=[d_{j0},d_{j1},\cdots,d_{jq_j}]^{\mathrm{T}}\in\boldsymbol{R}^{q_j+1} \tag{21}$$

$$\boldsymbol{f}_j(t)=[1,f_{j1}(t),\cdots,f_{jq_j}(t)]^{\mathrm{T}}\in\boldsymbol{R}^{q_j+1}\quad j=1,2,\cdots,p \tag{22}$$

Hence, the disturbance $\boldsymbol{d}(t)$ is expressed as

$$\boldsymbol{d}(t)=\boldsymbol{N}^{*\mathrm{T}}\boldsymbol{f}(t) \tag{23}$$

$$\boldsymbol{N}^{*\mathrm{T}}=\begin{bmatrix}\boldsymbol{\mu}_1^{*\mathrm{T}} & \boldsymbol{0}^{\mathrm{T}}_{(q_2+1)} & \cdots & \boldsymbol{0}^{\mathrm{T}}_{(q_p+1)} \\ \boldsymbol{0}^{\mathrm{T}}_{(q_1+1)} & \boldsymbol{\mu}_2^{*\mathrm{T}} & \cdots & \boldsymbol{0}^{\mathrm{T}}_{(q_p+1)}\ \boldsymbol{0}^{\mathrm{T}}_{(q_1+1)}\end{bmatrix}\in\boldsymbol{R}^{p\times q} \tag{24}$$

$$\boldsymbol{f}(t)=[\boldsymbol{f}_1^{\mathrm{T}}(t)\quad \boldsymbol{f}_2^{\mathrm{T}}(t)\quad\cdots\quad\boldsymbol{f}_p^{\mathrm{T}}(t)]^{\mathrm{T}}\in\boldsymbol{R}^q$$
$$q=q_1+q_2+\cdots+q_p+p \tag{25}$$

with $\boldsymbol{K}_{3d}^*=[K_{3d1}^*,K_{3d2}^*,\cdots,K_{3dp}^*],K_{3dj}^*\in\boldsymbol{R}^M,j=1,2,\cdots,p$, the disturbance rejection term $\boldsymbol{K}_3^{*\mathrm{T}}(t)$ is parameterized as

$$\boldsymbol{K}_3^*(t)=\boldsymbol{K}_{3d}^*\boldsymbol{d}(t)=\boldsymbol{K}_{3d}^*\boldsymbol{N}^{*\mathrm{T}}\boldsymbol{f}(t)=\boldsymbol{K}_{3f}^*\boldsymbol{f}(t) \tag{26}$$

where the parameter matrix is

$$K_{3f}^{*}=[\varphi_{31}^{*},\varphi_{32}^{*},\cdots,\varphi_{3p}^{*}]\in \boldsymbol{R}^{M\times q}$$

$$q=q_1+q_2+\cdots+q_p+p$$

$$\varphi_{3j}^{*}=\boldsymbol{K}_{3dj}^{*}\boldsymbol{\mu}_j^{*\mathrm{T}}\in \boldsymbol{R}^{M\times(q_j+1)}\quad j=1,2,\cdots,p \tag{27}$$

Next, the adaptive disturbance rejection design for the state feedback control scheme will be studied for the plant with uncertainties from the plant and unmatched disturbances.

2.3 Error equation

Applying Eq. (4) to the system in Eq. (2), the closed-loop system becomes

$$\begin{aligned}\dot{\boldsymbol{x}}(t)=&(\boldsymbol{A}+\boldsymbol{B}\boldsymbol{K}_1^{*\mathrm{T}})\boldsymbol{x}(t)+\boldsymbol{B}\boldsymbol{K}_2^{*}\boldsymbol{r}(t)+\\&\boldsymbol{B}\boldsymbol{K}_3^{*}(t)+\boldsymbol{B}_d\boldsymbol{d}(t)+\boldsymbol{B}[\boldsymbol{v}(t)-\\&\boldsymbol{K}_1^{*\mathrm{T}}\boldsymbol{x}(t)-\boldsymbol{K}_2^{*}\boldsymbol{r}(t)-\boldsymbol{K}_3^{*}(t)]\\ \boldsymbol{y}(t)=&\boldsymbol{C}\boldsymbol{x}(t)\end{aligned} \tag{28}$$

In view of Eq. (19) the output tracking error equation is

$$\begin{aligned}&\boldsymbol{e}(t)=\boldsymbol{y}(t)-\boldsymbol{y}_m(t)=\\&\boldsymbol{W}_m(s)\boldsymbol{K}_p^{*}[\boldsymbol{v}-\boldsymbol{K}_1^{*\mathrm{T}}\boldsymbol{x}-\boldsymbol{K}_2^{*}\boldsymbol{r}-\boldsymbol{K}_3^{*}](t)+\boldsymbol{f}_p(t)\\&\boldsymbol{K}_p^{*}=\boldsymbol{K}_2^{*-1}\end{aligned} \tag{29}$$

where $\boldsymbol{f}_p(t)=\boldsymbol{C}e^{(\boldsymbol{A}+\boldsymbol{B}\boldsymbol{K}_1^{*\mathrm{T}})t}\boldsymbol{x}(0)$ converges to zero exponentially fast due to the stability of $\boldsymbol{A}+\boldsymbol{B}\boldsymbol{K}_1^{*\mathrm{T}}$ and $\boldsymbol{W}_m(s)=\boldsymbol{\xi}_m^{-1}(s)$. Hence we have

$$\begin{aligned}&\boldsymbol{\xi}_m(s)[e](t)=\\&\boldsymbol{K}_p[\boldsymbol{v}(t)-\boldsymbol{K}_1^{*\mathrm{T}}\boldsymbol{x}(t)-\boldsymbol{K}_2^{*}\boldsymbol{r}(t)-\boldsymbol{K}_3^{*}(t)]\end{aligned} \tag{30}$$

2.4 Adaptive designs using LDU decomposition

To deal with the uncertainty of the high-frequency gain matrix $\boldsymbol{K}_p$, we use the LDU decomposition in Lemma 1, we have

$$\begin{aligned}&\boldsymbol{L}^{-1}\boldsymbol{\xi}_m(s)[e](t)=\\&\boldsymbol{D}\boldsymbol{U}[\boldsymbol{v}(t)-\boldsymbol{K}_1^{*\mathrm{T}}\boldsymbol{x}(t)-\boldsymbol{K}_2^{*}\boldsymbol{r}(t)-\boldsymbol{K}_3^{*}(t)]\end{aligned} \tag{31}$$

We have the following formation

$$\boldsymbol{U}\boldsymbol{v}(t)=\boldsymbol{v}(t)-(\boldsymbol{I}-\boldsymbol{U})\boldsymbol{v}(t) \tag{32}$$

with Eqs. (31), (32), we have

$$\begin{aligned}\boldsymbol{L}^{-1}\boldsymbol{\xi}_m(s)[e](t)=&\boldsymbol{D}[\boldsymbol{v}(t)-(\boldsymbol{I}-\boldsymbol{U})\boldsymbol{v}(t)-\\&\boldsymbol{U}(\boldsymbol{K}_1^{*\mathrm{T}}\boldsymbol{x}(t)-\boldsymbol{K}_2^{*}\boldsymbol{r}(t)-\boldsymbol{K}_3^{*}(t))]\end{aligned} \tag{33}$$

We have a new parameterization

$$\boldsymbol{L}^{-1}\boldsymbol{\xi}_m(s)[e](t)=\boldsymbol{D}[\boldsymbol{v}(t)-\boldsymbol{\Phi}_0^{*}\boldsymbol{v}(t)-\boldsymbol{\Phi}_1^{*\mathrm{T}}\boldsymbol{\omega}(t)] \tag{34}$$

where $\boldsymbol{\Phi}_1^{*\mathrm{T}}=[\boldsymbol{U}\boldsymbol{K}_1^{*\mathrm{T}},\boldsymbol{U}\boldsymbol{K}_2^{*},\boldsymbol{U}\boldsymbol{K}_{3f}^{*}]$ and $\boldsymbol{w}(t)=[\boldsymbol{x}^{\mathrm{T}}(t),\boldsymbol{R}^{\mathrm{T}}(t),\boldsymbol{f}^{\mathrm{T}}(t)]^{\mathrm{T}}$. This new parameterization motivates the new controller structure

$$\boldsymbol{v}(t)=\boldsymbol{\Phi}_0\boldsymbol{v}(t)+\boldsymbol{\Phi}_1^{\mathrm{T}}\boldsymbol{\omega}(t) \tag{35}$$

where $\boldsymbol{\Phi}_0$ and $\boldsymbol{\Phi}_1^{\mathrm{T}}$ are the estimates of $\boldsymbol{\Phi}_0^{*}$ and $\boldsymbol{\Phi}_1^{*\mathrm{T}}$, $\boldsymbol{\Phi}_0$ is the upper triangular with zero diagonal elements (only its nonzero elements are estimated). Matrix $\boldsymbol{\Phi}_0$ has the same strictly form as that of $\boldsymbol{\Phi}_0^{*}=(\boldsymbol{I}-\boldsymbol{U})$, and

$$\boldsymbol{\Phi}_0=\begin{bmatrix}0&\varphi_{12}&\varphi_{13}&\cdots\\0&0&\varphi_{23}&\cdots\\\vdots&\vdots&\vdots&\vdots\\0&0&\cdots&0\\0&0&\cdots&0\end{bmatrix}\in\boldsymbol{R}^{M\times M} \tag{36}$$

From Eqs. (34), (35), we obtain a new error model

$$\boldsymbol{\xi}_m(s)[e](t)+\boldsymbol{\Theta}_0^{*}\boldsymbol{\xi}_m(s)[e](t)=\boldsymbol{D}\widetilde{\boldsymbol{\Phi}}^{\mathrm{T}}(t)\bar{\boldsymbol{\omega}}(t) \tag{37}$$

where the parameter error is $\widetilde{\boldsymbol{\Phi}}(t)=\boldsymbol{\Phi}(t)-\boldsymbol{\Phi}^{*}$, and $\boldsymbol{\Phi}^{\mathrm{T}}(t)=[\boldsymbol{\Phi}_0(t),\boldsymbol{\Phi}_1^{\mathrm{T}}(t)]$ is the estimate of unknown parameter matrix $\boldsymbol{\Phi}^{*\mathrm{T}}=[\boldsymbol{\Phi}_0^{*},\boldsymbol{\Phi}_1^{\mathrm{T}}]$, $\bar{\boldsymbol{\omega}}(t)=[\boldsymbol{v}^{\mathrm{T}}(t),\boldsymbol{\omega}^{\mathrm{T}}(t)]^{\mathrm{T}}$ and $\boldsymbol{\omega}(t)=[\boldsymbol{x}^{\mathrm{T}}(t),\ \boldsymbol{R}^{\mathrm{T}}(t),\ \boldsymbol{f}^{\mathrm{T}}(t)]^{\mathrm{T}}$, where $\boldsymbol{\Phi}_0^{*}=(\boldsymbol{L}^{-1}-\boldsymbol{I})$ is introduced is introduced to parameterize the unknown matrix L, which has the special form

$$\boldsymbol{\Theta}_0^{*}=\begin{bmatrix}0&0&\cdots&0\\\theta_{21}^{*}&0&\cdots&0\\\vdots&\cdots&0&0\\\theta_{M1}^{*}&\cdots&\theta_{MM-1}^{*}&0\end{bmatrix}\in\boldsymbol{R}^{M\times M} \tag{38}$$

For such a matrix $\boldsymbol{\Phi}_0^{*}$, the parameter vectors defined as

$$\begin{aligned}&\theta_2^{*}=\theta_{21}^{*}\in R\\&\boldsymbol{\theta}_3^{*}=[\theta_{31}^{*},\theta_{32}^{*}]^{\mathrm{T}}\in\boldsymbol{R}^2\\&\vdots\\&\boldsymbol{\theta}_{M-1}^{*}=[\theta_{M-11}^{*},\cdots,\theta_{M-1M-2}^{*}]\in\boldsymbol{R}^{M-2}\\&\boldsymbol{\theta}_M^{*}=[\theta_{M1}^{*},\cdots,\theta_{MM-1}^{*}]\in\boldsymbol{R}^{M-1}\end{aligned} \tag{39}$$

and their estimates are

$$\begin{aligned}&\theta_2(t)=\theta_{21}(t)\in R\\&\boldsymbol{\theta}_3(t)=[\theta_{31}(t),\theta_{32}(t)]^{\mathrm{T}}\in\boldsymbol{R}^2\\&\vdots\\&\boldsymbol{\theta}_{M-1}(t)=[\theta_{M-11}(t),\cdots,\theta_{M-1M-2}(t)]\in\boldsymbol{R}^{M-2}\\&\boldsymbol{\theta}_m(t)=[\theta_{M1}(t),\cdots,\theta_{MM-2}(t)]\in\boldsymbol{R}^{M-1}\end{aligned} \tag{40}$$

We introduce a filter $\boldsymbol{h}(s)=\dfrac{1}{\boldsymbol{f}(s)}$ where $\boldsymbol{f}(s)$ is chosen as a stable and monic polynomial whose degree is equal to the maximum degree of the modified $\boldsymbol{\xi}_m(s)$. Operating both sides of Eq. (37) by $\boldsymbol{h}(s)\boldsymbol{I}_M$ leads to

$$\boldsymbol{\xi}_m(s)\boldsymbol{h}(s)[e](t)+\boldsymbol{\Theta}_0^*\boldsymbol{\xi}_m(s)\boldsymbol{h}(s)[e](t)=\boldsymbol{D}^*\boldsymbol{h}(s)[\widetilde{\boldsymbol{\Phi}}^{\mathrm{T}}\bar{\boldsymbol{\omega}}](t) \tag{41}$$

We defined

$$\bar{\boldsymbol{e}}(t)=\boldsymbol{\xi}_m(s)\boldsymbol{h}(s)[e](t)=[\bar{\boldsymbol{e}}_1(t),\cdots,\bar{\boldsymbol{e}}_m(t)]^{\mathrm{T}} \tag{42}$$

$$\boldsymbol{\eta}_i(t)=[\bar{\boldsymbol{e}}_1(t),\cdots,\bar{\boldsymbol{e}}_{i-1}(t)]^{\mathrm{T}}\in\boldsymbol{R}^{i-1}\quad i=2,3,\cdots,M \tag{43}$$

From Eqs. (41), (42) in Eq. (43), we obtained

$$\bar{\boldsymbol{e}}(t)+[\boldsymbol{0},\boldsymbol{\theta}_2^{*\mathrm{T}}(t)\boldsymbol{\eta}_2(t),\boldsymbol{\theta}_3^{*\mathrm{T}}(t)\boldsymbol{\eta}_3(t),\cdots,\boldsymbol{\theta}_m^{*\mathrm{T}}(t)\boldsymbol{\eta}_m(t)]^{\mathrm{T}}=\boldsymbol{D}\boldsymbol{h}(s)[\widetilde{\boldsymbol{\Phi}}^{\mathrm{T}}\bar{\boldsymbol{\omega}}](t) \tag{44}$$

Based on the parameterized error Eq. (41), an estimation error signal is introduced

$$\boldsymbol{\varepsilon}(t)=\bar{\boldsymbol{e}}(t)+[\boldsymbol{0},\boldsymbol{\theta}_2^{\mathrm{T}}(t)\boldsymbol{\eta}_2(t),\boldsymbol{\theta}_3^{\mathrm{T}}(t)\boldsymbol{\eta}_3(t),\cdots,\boldsymbol{\theta}_m^{\mathrm{T}}(t)\boldsymbol{\eta}_m(t)]^{\mathrm{T}}+\boldsymbol{\Psi}(t)\boldsymbol{\zeta}(t)\in\boldsymbol{R}^M \tag{45}$$

where $\boldsymbol{\Psi}(t)\in\boldsymbol{R}^{M\times M}$ is the estimate of $\boldsymbol{\Psi}^*=\boldsymbol{D}$ and

$$\boldsymbol{\zeta}(t)=\boldsymbol{h}(s)[\bar{\boldsymbol{\omega}}](t)\quad i=1,2,\cdots,M \tag{46}$$

$$\boldsymbol{\zeta}(t)=\boldsymbol{\Phi}^{\mathrm{T}}(t)\zeta(t)-\boldsymbol{h}(s)[\boldsymbol{\Phi}^{\mathrm{T}}\bar{\boldsymbol{\omega}}](t)\quad i=1,2,\cdots,M \tag{47}$$

Following Eqs. (41)—(47), here we have

$$\boldsymbol{\varepsilon}(t)=[\boldsymbol{0},\widetilde{\boldsymbol{\theta}}_2^{\mathrm{T}}\eta_2(t),\widetilde{\boldsymbol{\theta}}_3^{\mathrm{T}}\eta_3(t),\cdots,\widetilde{\boldsymbol{\theta}}_M^{\mathrm{T}}\eta_m(t)]^{\mathrm{T}}+\boldsymbol{D}\widetilde{\boldsymbol{\Phi}}^{\mathrm{T}}+\widetilde{\boldsymbol{\Psi}}(t)\boldsymbol{\zeta}(t) \tag{48}$$

where $\widetilde{\boldsymbol{\Psi}}(t)=\boldsymbol{\Psi}(t)-\boldsymbol{\Psi}^*$ and $\widetilde{\boldsymbol{\theta}}_{\boldsymbol{I}}(t)=\boldsymbol{\theta}_{\boldsymbol{I}}(t)-\boldsymbol{\theta}_{\boldsymbol{I}}^*$ are the parameter errors. This error model is a choice for update laws.

Based on the error model Eq. (48), the adaptive laws are chosen as

$$\dot{\boldsymbol{\theta}}_i(t)=-\frac{\boldsymbol{P}_{\theta_i}\boldsymbol{\varepsilon}_i(t)\boldsymbol{\eta}_i(t)}{\boldsymbol{m}^2(t)}\quad i=2,\cdots,M \tag{49}$$

$$\dot{\boldsymbol{\Phi}}^{\mathrm{T}}(t)=-\frac{\boldsymbol{P}_{\varphi}\boldsymbol{\varepsilon}(t)\boldsymbol{\zeta}^{\mathrm{T}}(t)}{\boldsymbol{m}^2(t)} \tag{50}$$

$$\dot{\boldsymbol{\Psi}}(t)=-\frac{\boldsymbol{P}\boldsymbol{\varepsilon}(t)\boldsymbol{\xi}^{\mathrm{T}}(t)}{\boldsymbol{m}^2(t)} \tag{51}$$

where $\boldsymbol{P}_{\theta i}=\boldsymbol{P}_{\theta i}^{\mathrm{T}}>0$, $i=2,3,\cdots,M$, and $\boldsymbol{P}=\boldsymbol{P}^{\mathrm{T}}>0$ are adaptive gains, $\boldsymbol{P}_{\varnothing}>0$ is defined in Eq. (7). $\boldsymbol{\varepsilon}(t)=[\varepsilon_1(t),\varepsilon_2(t),\cdots,\varepsilon_M(t)]^{\mathrm{T}}$ is calculated from Eq. (48), and

$$m^2(t)=1+\boldsymbol{\zeta}^{\mathrm{T}}(t)\boldsymbol{\zeta}(t)+\boldsymbol{\zeta}^{\mathrm{T}}(t)\boldsymbol{\zeta}(t)+\sum_{i=2}^{M}\boldsymbol{\eta}_i^{\mathrm{T}}\boldsymbol{\eta}_i(t) \tag{52}$$

2.5 Stability analysis

For the adaptive laws in Eqs. (49)—(51), we have the following desired stability properties.

Lemma 4[22] The adaptive laws ensures that

(1) $\boldsymbol{\theta}_i(t)\in\boldsymbol{L}^\infty$, $i=2,3,\cdots,M$; $\boldsymbol{\Phi}(t)\in\boldsymbol{L}^\infty$, $\boldsymbol{\Psi}(t)\in\boldsymbol{L}^\infty$, and $\dfrac{\boldsymbol{\varepsilon}(t)}{\boldsymbol{m}(t)}\in\boldsymbol{L}^2\cap\boldsymbol{L}^\infty$;

(2) $\dot{\boldsymbol{\theta}}_i(t)\in\boldsymbol{L}^2\cap\boldsymbol{L}^\infty$, $i=2,3,\cdots,M$, $\dot{\boldsymbol{\Phi}}(t)\in\boldsymbol{L}^2\cap\boldsymbol{L}^\infty$, and $\dot{\boldsymbol{\Psi}}(t)\in\boldsymbol{L}^2\cap\boldsymbol{L}^\infty$.

Proof

We choose the positive definition function

$$\boldsymbol{V}=\frac{1}{2}\{\sum_{i=2}^{M}\widetilde{\boldsymbol{\theta}}_i^{\mathrm{T}}\boldsymbol{\Gamma}_{\theta_i}^{-1}\tilde{\theta}+\mathrm{tr}[\widetilde{\boldsymbol{\Psi}}^{\mathrm{T}}\boldsymbol{\Gamma}^{-1}\widetilde{\boldsymbol{\Psi}}]+\mathrm{tr}[\widetilde{\boldsymbol{\Phi}}^{\mathrm{T}}\boldsymbol{D}\widetilde{\boldsymbol{\Phi}}]\} \tag{53}$$

From Eqs. (51), we derive the time-rivate of $\boldsymbol{V}$

$$\boldsymbol{V}=-\sum_{i=2}^{M}\frac{\widetilde{\boldsymbol{\theta}}_i^{\mathrm{T}}\boldsymbol{\varepsilon}_i(t)\boldsymbol{\eta}_i(t)}{\boldsymbol{m}^2(t)}-\frac{\boldsymbol{\xi}^{\mathrm{T}}(t)\widetilde{\boldsymbol{\Psi}}\boldsymbol{\varepsilon}(t)}{\boldsymbol{m}^2(t)}-\frac{\boldsymbol{\zeta}^{\mathrm{T}}(t)\widetilde{\boldsymbol{\Phi}}\boldsymbol{D}\boldsymbol{\varepsilon}(t)}{\boldsymbol{m}^2(t)}=-\frac{\boldsymbol{\varepsilon}^{\mathrm{T}}(t)\boldsymbol{\varepsilon}(t)}{\boldsymbol{m}^2(t)}\leqslant 0. \tag{54}$$

Similar to the case in Ref. [22], we derive that

$$\begin{aligned}&\boldsymbol{\theta}_i(t)\in\boldsymbol{L}^\infty\quad i=2,3,\cdots,M\\&\boldsymbol{\Phi}\in\boldsymbol{L}^\infty\\&\boldsymbol{\Psi}\in\boldsymbol{L}^\infty\quad\frac{\boldsymbol{\varepsilon}(t)}{\boldsymbol{m}(t)}\in\boldsymbol{L}^2\cap\boldsymbol{L}^\infty\\&\boldsymbol{\theta}_i(t)\in\boldsymbol{L}^2\cap\boldsymbol{L}^\infty\quad i=2,3,\cdots,M\\&\dot{\boldsymbol{\Phi}}(t)\in\boldsymbol{L}^2\cap\boldsymbol{L}^\infty\quad\dot{\boldsymbol{\Psi}}(t)\in\boldsymbol{L}^2\cap\boldsymbol{L}^\infty\end{aligned} \tag{55}$$

Based on Lemma 4, the following desired closed-loop system properties are established.

Theorem 2 For the plant (2) with uncertainties from the system parameters and disturbance (3) under Assumptions 1—4, and the reference model (5), the LDU decomposition based MRAC scheme with the adaptive controller (4) and adaptive parameter update laws in Eqs. (49)—(51) guarantees closed-loop system boundedness and asymptotic output tracking $\lim_{t\to\infty}\boldsymbol{e}(t)=0$ with $\boldsymbol{e}(t)=\boldsymbol{y}(t)-\boldsymbol{y}_m(t)$.

Proof (outline)

The proof of this stability theorem can be established through using a unified framework. Because the control input $\boldsymbol{v}(t)$ described in (35) depends on the state $\boldsymbol{x}(t)$, it first needs to be expressed by using the system output $\boldsymbol{y}(t)$ through establishing the state observer of the plant

$$\dot{\hat{\boldsymbol{x}}}(t)=(\boldsymbol{A}-\boldsymbol{LC})\hat{\boldsymbol{x}}(t)+\boldsymbol{Bv}(t)+\boldsymbol{B}_d\boldsymbol{d}(t)+\boldsymbol{Ly}(t) \tag{56}$$

where $\boldsymbol{L}\in\boldsymbol{R}^{n\times m}$ is a gain matrix such that $\boldsymbol{A}$-$\boldsymbol{LC}$ is stable, which is possible ($\boldsymbol{AC}$) is assumed to be detectable. Hence we have

$$\boldsymbol{v}(t)=\boldsymbol{\Phi}_1^{\mathrm{T}}(t)\boldsymbol{\omega}_1(t)+\boldsymbol{\Phi}_2^{\mathrm{T}}(t)\boldsymbol{\omega}_2(t)+\boldsymbol{\Phi}_{3d}^{\mathrm{T}}(t)\boldsymbol{\omega}_3(t)+\boldsymbol{K}_2(t)\boldsymbol{r}(t)+\boldsymbol{\Phi}_3(t)\boldsymbol{f}(t) \tag{57}$$

where $\boldsymbol{\Phi}_1^{\mathrm{T}}(t)$, $\boldsymbol{\Phi}_2^{\mathrm{T}}(t)$, $\boldsymbol{\Phi}_{3d}^{\mathrm{T}}(t)$, $\boldsymbol{K}_2^{\mathrm{T}}(t)$ and $\boldsymbol{\Phi}_3(t)$ are adaptive estimates of the corresponding nominal controller parameters and $\boldsymbol{\omega}_1(t)=\frac{\boldsymbol{a}(s)}{\boldsymbol{\Lambda}(s)}[v](t)$, $\boldsymbol{\omega}_2(t)=\frac{\boldsymbol{a}(s)}{\boldsymbol{\Lambda}(s)}[y](t)$, $\boldsymbol{\omega}_3(t)=\frac{\boldsymbol{b}(s)}{\boldsymbol{\Lambda}(s)}[f](t)$, with $\boldsymbol{a}(s)=[\boldsymbol{I}_M s\ \boldsymbol{I}_M \cdots s^{n-1}\ \boldsymbol{I}_M]^{\mathrm{T}}$, $\boldsymbol{b}(s)=[\boldsymbol{I}_q s\ \boldsymbol{I}_q \cdots s^{n-1}\ \boldsymbol{I}_q]^{\mathrm{T}}$, and $\boldsymbol{\Lambda}(s)=\frac{\boldsymbol{b}(s)}{\boldsymbol{\Lambda}(s)}[f](t)$ being a chosen monic stable polynomial of degree n, which has the same eigenvalues with $\boldsymbol{A}-\boldsymbol{LC}$. Then, introducing the fictitious filters for the plant $\boldsymbol{y}(t)=\boldsymbol{C}(s\boldsymbol{I}-\boldsymbol{A})^{-1}\boldsymbol{Bv}(t)+\boldsymbol{BC}(s\boldsymbol{I}-\boldsymbol{A})^{-1}\boldsymbol{B}_d\boldsymbol{d}(t)$ and using series transformations, the control input described as Eq. (57) is transformed into the form

$$\boldsymbol{v}(t)=\boldsymbol{G}_{11}(s,\cdot)[\bar{y}](t)+\boldsymbol{G}_{12}(s,\cdot)[r](t)+\boldsymbol{G}_{13}(s,\cdot)[f](t)+\boldsymbol{G}_{14}(s,\cdot)[\boldsymbol{f}_p](t) \tag{58}$$

where $\bar{y}(t)=\boldsymbol{h}(s)[y](t)$ ($\boldsymbol{h}(s)$ is given below Eq. (49)) and $\boldsymbol{G}_{11}(s,\cdot)$, $\boldsymbol{G}_{12}(s,\cdot)$, $\boldsymbol{G}_{13}(s,\cdot)$, and $\boldsymbol{G}_{14}(s,\cdot)$ are proper stable operators with finite gains. Furthermore, a filtered version of the output signal $\boldsymbol{y}(t)$ is expressed in a feedback framework

$$\|\bar{\boldsymbol{y}}(t)\|\leqslant x_0+\beta_1\int_0^t \boldsymbol{e}^{-\alpha_1(t-\tau)}x_1(\tau)\left(\int_0^\tau \boldsymbol{e}^{-\alpha_2(\tau-\omega)}\|\bar{\boldsymbol{y}}(\bar{\omega})\|\,\mathrm{d}\bar{\omega}\right)\mathrm{d}\tau \tag{59}$$

for some β_1, α_1, $\alpha_2>0$, and $x_1(t)=\|\bar{\boldsymbol{\Phi}}(t)\|+\|(t)\|\ \boldsymbol{m}(t)\in L^2\cap L^\infty$. Applying the small gain lemma to Eq. (59), we can conclude that $\bar{\boldsymbol{y}}(t)\in L^\infty$, and so $\boldsymbol{y}(t), \boldsymbol{v}(t)\in L^\infty$. Thus, the signals satisfy $\bar{\boldsymbol{\omega}}(t), \boldsymbol{\zeta}(t), \boldsymbol{\zeta}(t), \boldsymbol{m}(t), \boldsymbol{\varepsilon}(t)\in \boldsymbol{L}^\infty$. Furthermore, $\boldsymbol{\theta}_{\boldsymbol{l}}(t), \frac{\boldsymbol{\varepsilon}(t)}{\boldsymbol{m}(t)}, \bar{\boldsymbol{\Phi}}(t), \boldsymbol{\Psi}(t)\in \boldsymbol{L}^2$ (Lemma 4) are satisfied and in turn $\boldsymbol{\zeta}(t)$ and $\boldsymbol{e}(t)=\boldsymbol{y}(t)-\boldsymbol{y}_m(t)$, such that $\boldsymbol{e}(t)=\boldsymbol{y}(t)-\boldsymbol{y}_m(t)$ converges to zero.

3 Simulation

The proposed LDU decomposition based adaptive disturbance rejection scheme is used to an aircraft control system model with turbulence disturbances, and a detailed procedure is given.

3.1 Aircraft system model

The following example for a small passenger aircraft in a cruise configuration derived in Ref. [21], typical values of these parameters are

$$\boldsymbol{A}=\begin{bmatrix}0 & 0 & 1 & 0\\ 0.0487 & -0.0829 & 0 & -1\\ 0 & -4.546 & -1.699 & 0.1717\\ 0 & 3.382 & -0.0654 & -0.0893\end{bmatrix}$$

$$\boldsymbol{B}=\begin{bmatrix}0 & 0\\ 0 & 0.0116\\ 27.276 & 0.5758\\ 0.3952 & -1.362\end{bmatrix},\quad \boldsymbol{C}=\begin{bmatrix}1 & 0 & 0 & 0\\ 0 & 1 & 0 & 0\end{bmatrix}$$

$$\boldsymbol{B}_d=\begin{bmatrix}0 & 0\\ -0.0487 & 0.0829\\ 0 & 4.546\\ 0 & 3.382\end{bmatrix}$$

3.2 Controller design

For the aircraft system, the transfer function, $\boldsymbol{G}_p(s)=\boldsymbol{C}(s\boldsymbol{I}-\boldsymbol{A})^{-1}$ has stable zeros: $s_1=-4.507$, $s_2=-0.91$, $s_3=-0.5685$, and is strictly proper and full rank. The interactor matrix is chosen as

$$\boldsymbol{\xi}(s)=\mathrm{diag}\{s+1\quad (s+1)^2\} \tag{60}$$

The high-frequency matrix

$$\boldsymbol{K}_p=\lim_{s\to\infty}\boldsymbol{\xi}_m(s)\boldsymbol{G}_p(s)=\begin{bmatrix}2.2673 & 8.8455\\ -0.0902 & -0.3521\end{bmatrix} \tag{61}$$

is finite and nonsingular and the matrix

$$\boldsymbol{K}_d=\lim_{s\to\infty}\boldsymbol{\xi}_m(s)\boldsymbol{G}_d(s)=\begin{bmatrix}-0.0386 & -0.0526\\ -0.2481 & -0.6246\end{bmatrix} \tag{62}$$

is finite. We choose $\boldsymbol{h}(s)=\frac{1}{(s+1)^2}$. From $\boldsymbol{G}_p(s)$ and $\boldsymbol{G}_d(s)$, we can obtain

$$\lim_{s\to\infty}\boldsymbol{Z}_0^{-1}(s)\boldsymbol{Z}_d(s)=\begin{bmatrix}-0.017 & -0.0064\\ 2.7493 & 1.7739\end{bmatrix} \tag{63}$$

which means relative degree condition assumption 4 is ensured. The related gain parameters in adaptive laws in Eqs. (49)—(51) are chosen as

$$\boldsymbol{P}_\theta=5, \boldsymbol{P}_\varphi=\mathrm{diag}\{0.5\quad 0.5\}$$
$$P=\mathrm{diag}\{1\quad 1\} \tag{64}$$

3.3 Simulation results

Two types of disturbance are described the constant turbulence and the time-varying turbulence.

(1) We consider the constant roll and slide angle wind velocity disturbance as

$\varphi_w = 1$ crad/s, $\beta_w = 1$ crad/s, (cradiscent rad).

(2) The time-varying roll and slide angle windvelocity disturbance are as $\varphi_w = 2\sin(0.2t)$ crad/s, $\beta_w = 3\sin(0.2t) + 2\sin(0.5t)$ crad/s,

Three sets of simulation results are provided below.

Case 1 is for time-varying tracking with reference step input when the uncertainty parameters and constant roll and slide angle wind velocity disturbance occur. As shown in Figs. 1,2, the LQR controller is able to stabilize the perturbed dynamics and the tracking performance is unacceptable. The aileron and rudder deflections exhibit the unwanted oscillations. As shown in Figs. 3,4, the new MRAC method is able to stabilize the perturbed dynamics and recovers the desired closed-loop tracking performance and the transient of this controller is well performed.

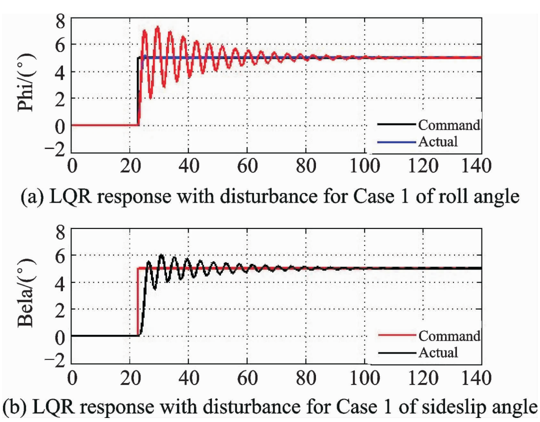

(a) LQR response with disturbance for Case 1 of roll angle

(b) LQR response with disturbance for Case 1 of sideslip angle

Fig. 1 LQR response with disturbance for Case 1

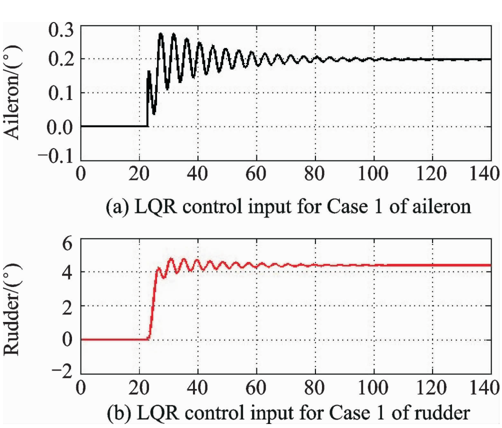

(a) LQR control input for Case 1 of aileron

(b) LQR control input for Case 1 of rudder

Fig. 2 LQR control input for Case 1

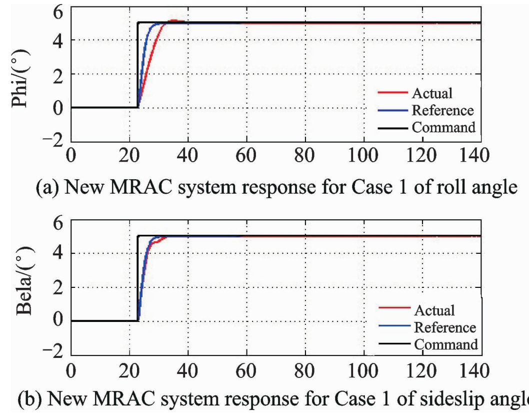

(a) New MRAC system response for Case 1 of roll angle

(b) New MRAC system response for Case 1 of sideslip angle

Fig. 3 New MRAC system response for Case 1

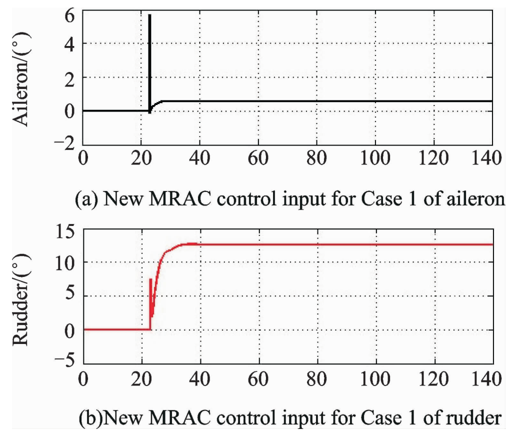

(a) New MRAC control input for Case 1 of aileron

(b)New MRAC control input for Case 1 of rudder

Fig. 4 New MRAC control input for Case 1

Case 2 is for the corresponding time-varying tracking with time-varying input

$$\boldsymbol{r}(t) = [\sin(0.3t) \quad 0.5\sin(2t)]^{\mathrm{T}}$$

when the uncertainty parameters and constant roll and slide angle wind velocity disturbance occur. As shown in Figs. 5,6, the proposed controller is able to stabilize the perturbed dynamics and recovers the desired closed-loop tracking performance.

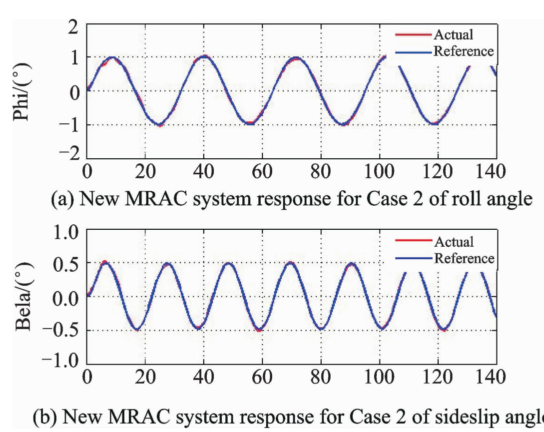

(a) New MRAC system response for Case 2 of roll angle

(b) New MRAC system response for Case 2 of sideslip angle

Fig. 5 New MRAC system response for Case 2

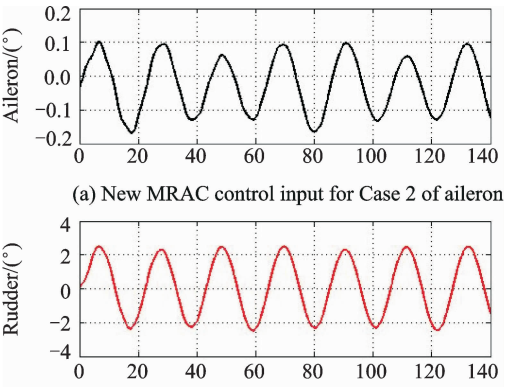

(a) New MRAC control input for Case 2 of aileron
(b) New MRAC control input for Case 2 of rudder

Fig. 6 New MRAC control input for Case 2

Case 3 is for corresponding time-varying tracking tracking with time-varying input $\boldsymbol{r}(t) = [\sin(0.3t) \quad 0.5\sin(2t)]^{\mathrm{T}}$ when time-varying roll and slide angle wind velocity disturbance occur. As shown in Figs. 7, 8, we can also draw the same conclusions as Case 2.

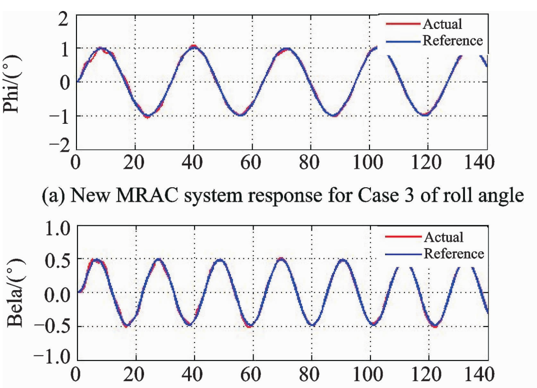

(a) New MRAC system response for Case 3 of roll angle
(b) New MRAC system response for Case 3 of sideslip angle

Fig. 7 New MRAC system response for Case 3

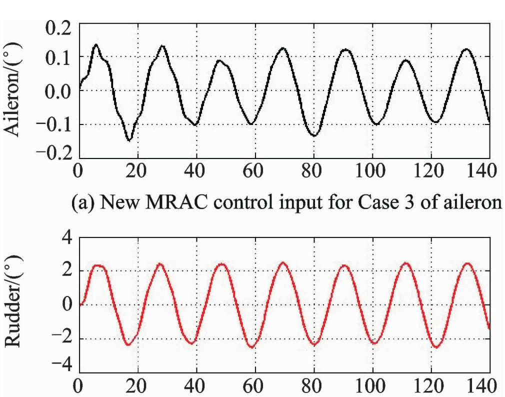

(a) New MRAC control input for Case 3 of aileron
(b) New MRAC control input for Case 3 of rudder

Fig. 8 New MRAC control input for Case 3

From the simulations above, the proposed new controller shows great effectiveness when the matched and unmatched disturbance occur.

4 Conclusions

In this paper, a multivariable disturbance rejection scheme is presented to solve the wind turbulence problem. The state feedback output tracking MRAC scheme is designed based on the LDU decomposition of the high-frequency gain matrix. The proposed LDU decomposition based disturbance rejection techniques are used to solve a typical aircraft turbulence compensation problem. Finally, simulation results have been presented to show that MRAC-based disturbance rejection scheme is an effective method of the aircraft control system with the disturbances.

References:

[1] ZHANG Y X, WANG Q, DONG C Y, et al. H_∞ output tracking control for flight control systems with time-varying delay [J]. Chinese Journal of Aeronautics, 2013, 26(5): 1251-1258.

[2] ZHU J, KHAYATI K. Adaptive sliding mode control convergence and gain boundedness revisited [J]. International Journal of Control, 2015, 89(4): 801-814.

[3] ZHANG J H, SHI P, LIN W G. Extended sliding mode observer based control for Markovian jump linear systems with disturbances [J]. Automatica, 2016, 70(3): 140-147.

[4] LI F B, WU L G, SHI P, et al. State estimation and sliding mode control for semi-Markovian jump systems with mismatched uncertainties [J]. Automatica, 2015, 51(1): 385-393.

[5] CASTANOS F, FRIDMAN L. Analysis and design of integral sliding manifolds for systems with unmatched perturbations [J]. IEEE Trans on Automatic Control, 2006, 51(5): 853-858.

[6] TAO G. Multivariable adaptive control: A survey [J]. Automatica, 2014, 50(11): 2737-2764.

[7] NARENDRA K, ANNASWAMY A. A new adaptive law for robust adaptation without persistent excitation [J]. IEEE Trans on Automatic Control, 1987, 32(2): 134-145.

[8] NGUYEN N T, BALAKRISHNAN S N. Bi-objective optimal control modification adaptive control for systems with input uncertainties [J]. IEEE/CAA Journal of Automatica Sinica, 2014, 1(4): 423-434.

[9] NGUYEN N T. Optimal control modification for robust adaptive control with large adaptive gain [J].

Systems & Control Letters, 2012, 61(4): 485-494.

[10] WIESE D P, ANNASWAMY A M. Adaptive control for a generic hypersonic vehicle [C]// Proc of AIAA Guidance, Navigation, and Control Conference. Boston: AIAA, 2013:1-21.

[11] PETERSON B, NARENDRA K. Bounded error adaptive control [J]. IEEE Trans on Automatic Control, 1982, 27(4): 1161-1168.

[12] IOANNOU P, TSAKALIS K. A robust direct adaptive controller [J]. IEEE Trans on Automatic Control, 1986, 31(11): 1033-1043.

[13] WANG Y, LI F, RONCH A D. Adaptive feedforward control design for gust loads alleviation of highly flexible aircraft [C]// Proc. of AIAA Atmospheric Flight Mechanics Conference. Dallas: AIAA, 2015: 1-22.

[14] SHAHSAVARI B, PAN J, HOROWITZ R. Adaptive rejection of periodic disturbances acting on linear systems with unknown dynamics [C]// Proc of IEEE Conference on Decision and Control. Las Vegas: AIAA, 2016:1-8.

[15] DYDEK Z T, ANNASWAMY A M, LAVRETSKY E. Adaptive control and the NASA X-15-3 flight revisited [J]. IEEE Control Systems, 2010, 30(3): 32-48.

[16] WIESE D P, ANNASWAMY A M, MUSE J, et al. Adaptive output feedback based on closed-loop reference models for hypersonic vehicles [J]. Journal of Guidance, Control, and Dynamics, 2015, 38(12): 2429-2440.

[17] LAVRETSKY E, GADIENT R, GREGORY I M. Predictor-based model reference adaptive control [J]. Journal of Guidance, Control, and Dynamics, 2010, 33(4): 1195-1201.

[18] ZENG J, Moulin B. Adaptive feedforward control for gust load alleviation [J]. Journal of Guidance, Control, and Dynamics, 2010, 33(3): 862-872.

[19] ZHENG F Y, GONG H J, ZHEN Z Y. Tradeoff analysis of the longitudinal carrier landing performance affecting factors for small UAV based on backstepping controller [J]. Transaction of Nanjing University of Aeronautics and Astronautics, 2015, 32(1):97-109.

[20] ZHENG F Y, GONG H J, WANG X H. Small carrier UAV lateral autonomous landing system [J]. Journal of Nanjing University of Aeronautics and Astronautics 2013,45(1):82-87. (in Chinese)

[21] LAVRETSKY E, WISE K A. Robust and adaptive control with aerospace applications [M]. New York: Springer, 2013.

[22] TAO G. Adaptive control design and analysis [M]. New Jersey: Wiley-Interscience, 2003.

Mr. **Wang Xin** received his B. S. and M. S. degrees in the College of Automation Engineering, Nanjing University of Aeronautics & Astronautics in 2005 and 2008, respectively. He is currently working toward Ph. D. degree in the College of Automation Engineering, Nanjing University of Aeronautics & Astronautics. His research interests include control theory, unmanned aerial vehicle control technology and flight control system.

Prof. **Chen Xin** received his Ph. D. degree in Northwestern Polytechnical University in 1996. He is now a professor in the College of Automation Engineering, Nanjing Univerisity of Aeronautics & Astronautics. His research interests include adaptive control, unmanned aerial vehicle control technology and flight control system.

Ms. **Wen Liyan** received her B. S. degree in Shandong University in 2009 and received her M. S. degree in Nanjing Normal University in 2012. She is currently working toward Ph. D. degree in the College of Automation Engineering, Nanjing University of Aeronautics & Astronautics. Her research interests include adaptive control, disturbance rejection and aircraft flight control.

(Executive Editor: Zhang Bei)